

# Neural Window Decoder for SC-LDPC Codes

Dae-Young Yun, *Member, IEEE*, Hee-Youl Kwak, *Member, IEEE*, Yongjune Kim, *Member, IEEE*, Sang-Hyo Kim, *Member, IEEE*, and Jong-Seon No, *Fellow, IEEE*

**Abstract**—In this paper, we propose a neural window decoder (NWD) for spatially coupled low-density parity-check (SC-LDPC) codes. The NWD augments the conventional window decoder (WD) by incorporating trainable neural weights. To improve both performance and complexity, we train these weights using three novel training strategies. First, we design a compact neural network that focuses training on the target nodes of the NWD. This target-specific training improves decoding performance while reducing complexity. Second, we introduce a non-uniform scheduling method for check node (CN) updates by learning trainable damping factors. These factors reflect the relative importance of CN updates, allowing the decoder to skip less critical updates. Finally, we address the error propagation (EP) problem inherent in SC-LDPC codes by introducing an EP-resilient weight set trained under EP scenarios. When an error is detected in the previous decoding window, the adaptive NWD switches to the EP-resilient weight set. For a practical SC-LDPC code of length 20000, the proposed NWD achieves a threefold improvement in decoding performance or a 45% reduction in decoding complexity, without altering the hardware-friendly decoding architecture.

**Index Terms**—Decoding schedules, deep learning, error propagation, low-density parity-check (LDPC) codes, neural decoder, spatially coupled LDPC (SC-LDPC) codes, window decoding.

## I. INTRODUCTION

THE recent emergence of machine learning technologies has significantly impacted a broad area of technological fields. This influence is also prominent in the field of communications, spanning topics such as channel estimation [1], end-to-end communication [2], [3], and channel coding [4]–[8]. Particularly, the application of deep learning techniques to the channel coding problem has marked a significant milestone [7]. The pioneering work [8] has introduced *neural decoders* that integrate iterative decoding algorithms, such as belief propagation (BP) and min-sum (MS) algorithms, with deep neural networks. These neural decoders introduce trainable weights to attenuate messages and mitigate the detrimental impact of short cycles.

In an effort to enhance the performance of neural decoders, a variety of machine learning techniques have been leveraged. Hyper-graph networks are incorporated into the neural network architecture to expand the model capacity [9]. Additionally,

D.-Y. Yun and H.-Y. Kwak are with the Department of Electrical, Electronic and Computer Engineering, University of Ulsan, Ulsan 44610, South Korea (e-mail: dyun95@gmail.com; ghy1228@gmail.com).

Y. Kim is with the Department of Electrical Engineering at Pohang University of Science and Technology (POSTECH), Pohang, Gyeongbuk 37673, South Korea (e-mail: yongjune@postech.ac.kr).

S.-H. Kim is with the Department of Electrical and Computer Engineering, Sungkyunkwan University, Suwon 16419, South Korea (e-mail: iamshkim@skku.edu).

J.-S. No is with the Department of Electrical and Computer Engineering, INMC, Seoul National University, Seoul 08826, South Korea (e-mail: jsno@snu.ac.kr).

the active learning technique [10], which involves the careful selection of effective training data, and the pruning method [11] are utilized to improve the performance of neural decoders. Recently, the boosting learning technique has been applied to address the error-floor issue of low-density parity-check (LDPC) codes [12], [13]. Another distinctive approach to enhance the performance of neural decoders is simplifying the training problem. For instance, the concept of recurrent neural networks is employed in neural decoders [14], resulting in a reduction of the number of training parameters. Similarly, various weight sharing techniques such as spatial [15], protograph [16], and degree-based sharing [17] have been proposed. This approach, by leveraging domain-specific knowledge and structural constraints, effectively reduces the search space that the model needs to explore during training. This not only leads to a significant reduction in training complexity and memory requirements but also allows the model to converge to a better solution, ultimately enhancing decoding performance.

With these efforts, neural decoders have gained recognition for their practicality and have been applied to various code classes, including algebraic [9], [18], LDPC [12], [13], [15], [19], generalized LDPC [20], and polar codes [21]. However, neural decoders have not yet been applied to one of the key counterparts of LDPC codes, namely, the spatially coupled LDPC (SC-LDPC) codes.

SC-LDPC codes, first introduced in [22], have attracted attention due to the threshold saturation effect, where their BP thresholds approach the optimal maximum a posteriori (MAP) thresholds of uncoupled block LDPC codes [23]. SC-LDPC codes are constructed by coupling  $L$  disjoint LDPC blocks in a repetitive structure. This recurrent form enables a unique decoding known as window decoding [24], [25]. The window decoder (WD) operates on a subgraph block, referred to as a window, aiming to decode target variable nodes (VNs) in each block. After decoding within the first window is completed, the process advances to the subsequent window and continues across all  $L$  blocks. Compared to the BP decoding, the WD offers advantages in terms of decoding latency, complexity, and memory requirements.

There are two important research directions for the WD. First, non-uniform scheduling is proposed to reduce decoding complexity [26]. Due to the unique structure of SC-LDPC codes, each CN update impacts the decoding process differently. The method in [26] computes a soft bit error rate (BER) estimation during the decoding process and omits CN updates that are expected to have a lesser impact on decoding. However, this method requires online computation of soft BERs during decoding, which introduces additional overhead. Second, an adaptive decoding strategy [27], [28] and the doping method [29] have been proposed to prevent error

propagation (EP) of WD. A decoding failure in one window can adversely affect subsequent decoding, potentially leading to a long chain of errors, called EP [30], [31]. The adaptive decoding strategy [27], [28] adjusts the number of iterations or window size, whereas the doping method [29] modifies the decoding or encoding processes. However, these approaches have drawbacks of requiring online BER estimation or modifying the code and decoder structures.

### A. Main Contributions of This Work

To improve WD in terms of performance, complexity, and robustness to EP, we propose a *neural window decoder* (NWD) and associated decoding strategies. The NWD operates in the same manner as the conventional WD but incorporates trainable weights. To the best of our knowledge, NWD is the first neural decoder specifically designed for SC-LDPC codes. In this paper, we present three primary contributions:

- 1) *Target-specific training*: We train the NWD using target-specific training, wherein the loss function only includes target VNs in the window. By restricting the network's output to the subset of VNs, the neural network is pruned, thereby allowing the omission of certain weights. We show that target-specific training converges faster with fewer trainable parameters and achieves a threefold improvement in decoding performance compared to the conventional WD. To ensure effective training of NWD, active learning [10] and normalized validation error [6] are also employed.
- 2) *Neural non-uniform scheduling*: We introduce neural non-uniform scheduling to further reduce the complexity of the NWD. Specifically, we train the NWD with trainable damping factors, which mix the current CN update result with the previous CN message to derive the current CN message. A large damping factor indicates that the current update is less important for decoding. Based on this metric, we propose a systematic method to determine the non-uniform scheduling of the NWD, and achieve 45% reduction in decoding complexity without performance degradation compared to the WD. This scheduling method enables flexible performance-complexity trade-offs.
- 3) *Adaptive NWD*: We propose an adaptive NWD scheme to mitigate EP of the NWD. We collect EP-inducing samples and train a specialized weight set, called the EP-resilient weight set, for EP scenarios. When a decoding failure is detected in the previous window, the adaptive NWD scheme employs the EP-resilient weight set for the current window; otherwise, it utilizes the plain weight set. The proposed adaptive scheme successfully reduces the EP probability without modifying the code or decoder structure or online BER estimation, offering an advantage over previous methods [27]–[29].

Note that all three contributions stem from the distinctive structure of SC-LDPC codes and WD, and they are tightly interrelated through the training of NWD. The overall algorithm of this work is summarized in Algorithm 1.

The rest of the paper is organized as follows. Section II introduces the notation and background. In Section III, we present the structure of NWD and target-specific training of

---

### Algorithm 1 Proposed Neural Window Decoder (NWD)

---

**Input:** Window size  $W$ , target size  $T$ , maximum number of iterations  $\bar{\ell}$ , number of CN updates to be skipped  $R$

1: **Target-specific training (Section III):**

- Build the neural network corresponding to a window with  $W$  and  $\bar{\ell}$ .
- Set the loss term to include only target nodes from positions 1 to  $T$ .
- Train the CN weights  $w_C^{(\ell)}$  using actively collected samples [10] and normalized validation error [6].

2: **Neural non-uniform scheduling (Section IV):**

- Train NWD with damping factors  $\gamma_C^{(\ell)}$ .
- Quantify the importance of each CN update based on the trained  $\gamma_C^{(\ell)}$ .
- Skip  $R$  CN updates with low importance from the decoding process.

3: **Adaptive NWD (Section V):**

- Build the NWD to incorporate the messages passed from the previous windows.
- Collect the training data using the boosting learning technique [13].
- Train the EP-resilient weight set  $\bar{w}_C^{(\ell)}$ .
- If an error is not detected in the previous window, apply the plain weight set  $w_C^{(\ell)}$ .
- Else, apply the EP-resilient weight set  $\bar{w}_C^{(\ell)}$ .

---

NWD. In Section IV, we describe the neural non-uniform scheduling based on the training results of damping factors. The adaptive NWD, which selectively uses the EP-resilient weight set based on the previous window stage, is presented in Section V. Finally, the conclusion is given in Section VII.

## II. PRELIMINARIES

### A. SC-LDPC Codes and Window Decoding

In this paper, we consider protograph-based SC-LDPC codes [32]. The protograph of SC-LDPC codes is constructed by the edge-spreading technique to couple every  $w$  adjacent LDPC blocks out of a total of  $L$  disjoint LDPC blocks into a single coupled chain. The parameters  $w$  and  $L$  are called coupling width and chain length, respectively. The base matrix  $\mathbf{B}$  consists of VNs at  $L$  positions and CNs at  $L+w$  positions; each position contains  $N$  protograph VNs and  $M$  protograph CNs. By lifting this base matrix with a factor of  $z$ , an SC-LDPC code is constructed with  $Ln = LNz$  VNs and  $(L+w)m = (L+w)Mz$  CNs, where  $n$  and  $m$  are the number of VNs and CNs at each position. Consequently, the code rate is given as

$$\mathcal{R} = 1 - \frac{(L+w)m}{Ln} = \left(1 - \frac{M}{N}\right) - \frac{M}{N} \frac{w}{L}.$$

When the uncoupled LDPC blocks possess regular VN and CN degrees of  $d_v$  and  $d_c$ , respectively, the resulting SC-LDPC codes are referred to as  $(d_v, d_c)$ -regular SC-LDPC codes. The protograph of the  $(3, 6)$ -regular SC-LDPC code is shown in

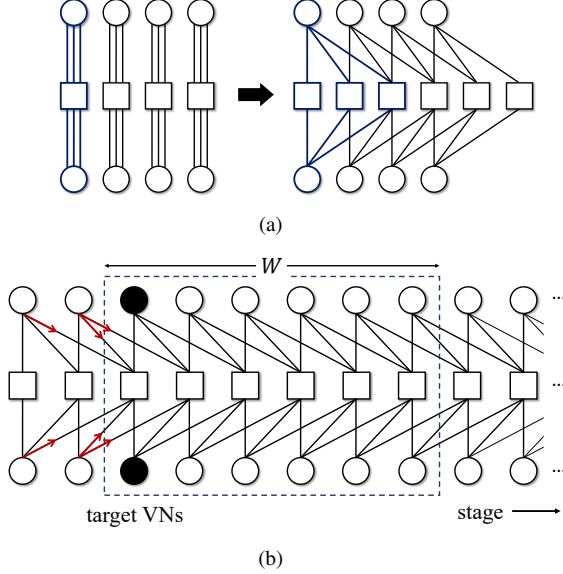


Fig. 1. (a) A photograph of the  $(3, 6)$ -regular SC-LDPC code with  $w = 2$  and  $L = 4$  constructed by the edge-spreading technique (b) window decoding with window size  $W = 6$  and target size  $T = 1$ . The dotted box indicates the window at the third stage, where the VNs in the first  $T$  positions in the window serve as target VNs (dark-filled nodes), and the previous target VNs transmit their decision LLRs (arrows).

Fig. 1(a), which will be used as a running example throughout this paper.

The repetitive structure of SC-LDPC codes facilitates sliding window decoding that operates within a window of size  $W$ , aiming to decode target VNs in the first  $T$  positions of the window [24]. Fig. 1(b) illustrates window decoding with  $W = 6$  and  $T = 1$ . Over the additive white Gaussian noise (AWGN) channel, the conventional WD proceeds as follows: The first stage begins within the window, which includes VNs and CNs at positions  $1, \dots, W$ . Decoding utilizes either the BP (sum-product) algorithm or the MS algorithm. The  $n$  target VNs in the first position are decoded based on their decision log-likelihood ratios (LLRs). Subsequently, the window shifts one position to the right, and the second stage begins. This process is repeated  $L$  times until all  $Ln$  VNs in the entire chain are decoded. From the second stage onward, the previously decoded VNs outside the window pass their decision LLRs, determined in the earlier stages, to the CNs in the current window (see the arrows in Fig. 1(b)).

In window decoding, if any  $n$  target VNs within a window stage retain bit errors after decoding, a block error is declared for that stage. Consequently, the block error rate (BLER) for SC-LDPC codes is defined as the rate of decoding failures for each target position. A frame error is declared when the decoded code frame of length  $Ln$  contains one or more bit errors after decoding the entire chain. The frame error rate (FER) refers to the proportion of frames with errors. While FER is the conventional reliability metric for frame-based transmissions, BLER is also practically important in applications such as real-time services, where the correct recovery of each block directly affects user experience.

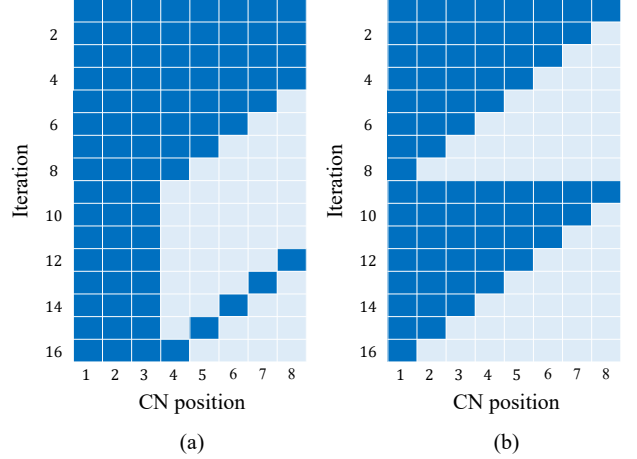


Fig. 2. Examples of the non-uniform decoding schedules of a  $(3, 6)$ -regular SC-LDPC code with  $W = 8$ ,  $\bar{l} = 16$  using (a) soft BER based method and (b) pragmatic method [26]. CN updates are only performed in the schedules with bold colors.

### B. Decoding Schedules for SC-LDPC Codes

Due to the iterative nature of message-passing decoding for LDPC codes, various message update schedules have been proposed to accelerate decoding convergence and reduce complexity [33]–[35]. The uniform parallel (flooding) schedule updates all VNs and CNs simultaneously. In contrast, the uniform serial schedule processes CNs in sequence, allowing VNs to immediately utilize the newly updated CN messages [33]. Both uniform schedules guarantee that all nodes are updated at least once in each iteration. On the other hand, non-uniform schedules, such as residual BP [34] and node-wise scheduling [35], dynamically change the update order within each iteration. This results in a varying number of updates for each node by the end of the decoding process.

Unlike in block LDPC codes, uniform serial schedules are less effective at reducing complexity in the window decoding of SC-LDPC codes [33]. To address this, several non-uniform schedules specifically suited for window decoding are proposed in [26]. The first scheme estimates soft BER at each iteration and skips CN updates with negligible impact, reusing their previous messages; it eliminates roughly 50% of CN updates but incurs significant real-time BER estimation overhead (Fig. 2(a)). Its pragmatic variant removes this overhead by presetting a fixed CN update scheduling: after an initial full update, the decoder skips one CN per iteration, starting with the furthest from the target and repeating every  $W$  iterations (Fig. 2(b)). This static schedule cuts CN updates by 35% without additional computation.

### C. Error Propagation in Window Decoding

As shown in Fig. 1(b), the decoding of the current window is influenced by the decision LLRs of previously processed VNs. Consequently, errors from prior stages can propagate, leading to a long chain of errors. EP is more prevalent in low-latency decoding settings that use a small window size  $W$  and a low maximum number of iterations  $\bar{l}$ . While

these configurations are favorable for reducing latency, they also increase the likelihood of block errors and EP. The presence of EP significantly worsens the BLER, especially when transmitting long or unterminated chains [30], [31].

To gain a deeper understanding of EP, a general Markov decoder model has been introduced in [29]. State  $S_i$  denotes  $i$  consecutive block errors before the current window. Transition probabilities obey  $q_{J-1} \geq q_{J-2} \geq \dots \geq q_0$ , reflecting the higher EP probability as the chain lengthens. This implies that the higher the value of  $i$ , the more severe the EP becomes. Therefore, it is crucial to tackle EP when  $i$  is small, at the early stages of propagation.

#### D. Neural Min-Sum Decoding

In this paper, we employ the neural MS decoding algorithm [36], which offers practical implementation with low decoding complexity while achieving superior performance. Let  $m_{v \rightarrow c}^{(\ell)}$  ( $m_{c \rightarrow v}^{(\ell)}$ ) denote the message passed from VN  $v$  to CN  $c$  (and vice versa) during the  $\ell$ -th iteration. Initially, these messages are set as  $m_{v \rightarrow c}^{(0)} = m_v^{\text{ch}}$ ,  $m_{c \rightarrow v}^{(0)} = 0$ , where  $m_v^{\text{ch}}$  represents the channel LLR of VN  $v$ . For iteration  $\ell = 1, 2, \dots, \bar{\ell}$ , the neural MS algorithm updates the messages as follows:

$$m_{v \rightarrow c}^{(\ell)} = m_v^{\text{ch}} + \sum_{c' \in \mathcal{N}(v) \setminus c} m_{c' \rightarrow v}^{(\ell-1)} \quad (1)$$

$$m_{c \rightarrow v}^{(\ell)} = w_{c \rightarrow v}^{(\ell)} \left( \prod_{v' \in \mathcal{N}(c) \setminus v} \text{sgn} \left( m_{v' \rightarrow c}^{(\ell)} \right) \right) \min_{v' \in \mathcal{N}(c) \setminus v} |m_{v' \rightarrow c}^{(\ell)}|, \quad (2)$$

where  $\mathcal{N}(v)$  denotes the neighbors of node  $v$ . We refer to  $w_{c \rightarrow v}^{(\ell)}$  as CN weights as they attenuate CN messages. At the last iteration, the decision LLR  $m_v^o$  of VN  $v$  is calculated as

$$m_v^o = m_v^{\text{ch}} + \sum_{c' \in \mathcal{N}(v)} m_{c' \rightarrow v}^{(\bar{\ell})}.$$

Unlike the weighted MS algorithm, which uses a heuristically optimized single weight, the neural MS algorithm employs a set of weights that are optimized through machine learning techniques within a neural network. The neural network is constructed from the Tanner graph of linear codes. While the neural MS algorithm demonstrates superior performance compared to the weighted MS algorithm, assigning distinct weights to every edge incurs significant memory requirements. To address this, various weight sharing techniques have been proposed, such as spatial sharing [15], photograph sharing, and CN sharing [16].

In this work, we train the neural MS decoders for 1000 epochs using the Adam optimizer [37], with 10000 samples per epoch drawn from multiple SNR points. Detailed training methods are provided in Section III-B.

### III. NEURAL WINDOW DECODER FOR SC-LDPC CODES

In this section, we propose the NWD and its training methods. The trained NWD achieves superior performance to conventional neural decoders with lower complexity.

#### A. Target-Specific Training of the NWD

Fig. 3 shows a part of the Tanner graph included in the first window with  $W = 3$  and  $z = 1$ , together with the neural network obtained by unrolling the Tanner graph for  $\bar{\ell} = 2$ . The network consists of  $Wn$  input and output nodes, along with  $2 \times \bar{\ell}$  hidden layers. The hidden-layer nodes correspond to the edges of the Tanner graph; odd and even layers perform VN and CN message updates in (1) and (2), respectively.

It should be noted that since the window configuration is repeated at each stage, training the weights in a single independent window is sufficient for all subsequent stages. Therefore, we train the NWD only for one independent window block. The trained weights can be reused across the entire chain of long SC-LDPC codes, requiring only a small number of weights. This weight-sharing property is a unique advantage of applying neural weights to window decoders over block decoders.

For photograph-based SC-LDPC codes, we employ two weight sharing techniques to facilitate training. Photograph weight sharing [16] ties weights on edges from the same protograph edge, reducing trainable weights by  $1/z$ . Additionally, CN weight sharing [16] unifies weights assigned to the same proto CN, representing CN weights as  $w_C^{(\ell)}$  for proto CN  $C$  and reducing the number of weights to  $W\bar{\ell}$ .

We use the BLER loss [39] (1 if any block error, else 0) for training, since perfect block decoding per window is needed to prevent EP. Conventional all-inclusive training includes all output VNs in the loss function:

$$L_A = \frac{1}{2} \left[ 1 - \text{sgn} \left( \min_{1 \leq v \leq Wn} m_v^o \right) \right].$$

On the other hand, we employ target-specific training for NWD, restricting the loss to the first  $T$  positions:

$$L_T = \frac{1}{2} \left[ 1 - \text{sgn} \left( \min_{1 \leq v \leq Tn} m_v^o \right) \right]. \quad (3)$$

Target-specific training results in structured pruning. In Fig. 3,  $T = 1$  target-specific training removes the output  $v_3 - v_6$  and the fourth-layer  $e_7 - e_{12}$  along with all nodes connected to them down to the input layer. In this example, target-specific training eliminates 47% of nodes and 43% of edges.

As the edges of the neural network are pruned, the associated CN weights are also removed. In Fig. 4, we plot the ratio between the number of trainable weights for target-specific training and that for all-inclusive training according to the window size  $W$  and  $\bar{\ell}$ . As shown in Fig. 4, a larger window size and a smaller maximum number of iterations lead to a greater reduction in weights. For example, with  $W = 18$  and  $\bar{\ell} = 4$ , the weight ratio is 0.3, indicating that target-specific training reduces the number of weights by 70%. In other words, target-specific training provides greater benefits in low-latency decoding scenarios, which involve using a small number of iterations to minimize decoding delay. Moreover, a larger window size is recommended to compensate for the performance loss from fewer iterations and prevent EP [25], [40]. Therefore, Fig. 4 shows that target-specific training is particularly advantageous in practical low-latency decoding scenarios.

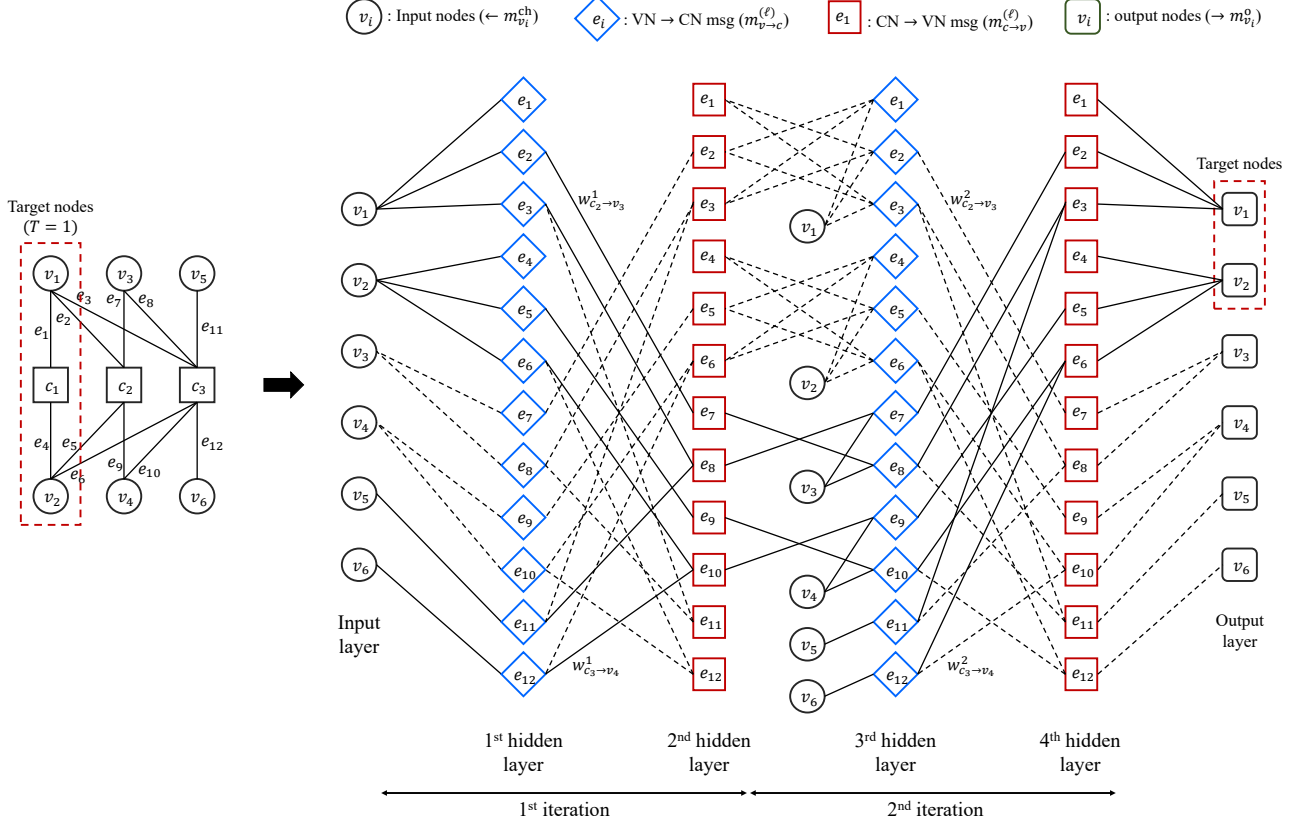


Fig. 3. A code within a window with  $W = 3$  and  $\bar{\ell} = 2$  is mapped to the neural network for training the NWD. The dashed lines in the network represent the edges that are included for all-inclusive training but are pruned for target-specific training.

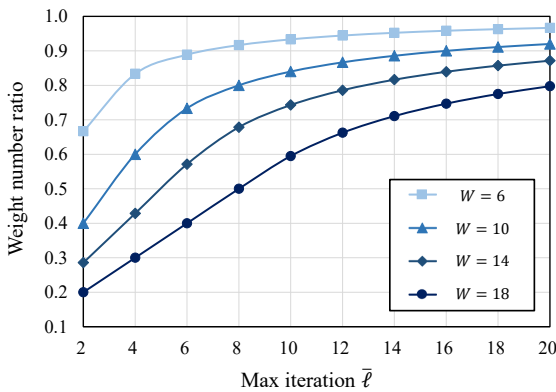


Fig. 4. Ratio between the numbers of trainable weights for target-specific training and all-inclusive training. A smaller ratio indicates a greater complexity reduction effect achieved by target-specific training.

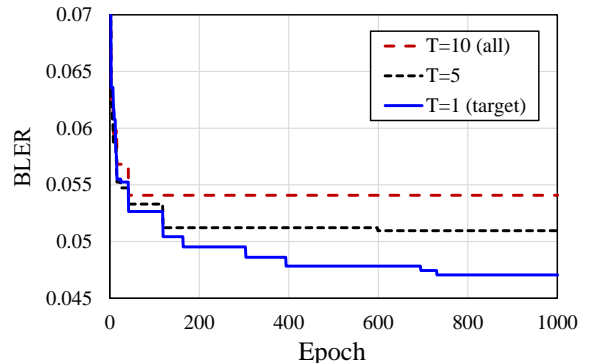


Fig. 5. Evolution of BLER over training epochs for NWD with different target sizes  $T$ .

fewer parameters.

### B. Training Techniques to Prevent Bias

Since the initial study on neural decoders by [8], most subsequent approaches have followed a similar training procedure: Each mini-batch contains samples drawn from multiple SNR points. An epoch is trained over these mini-batches, and validation is performed using held-out samples from the same SNR points. The final weights are selected from the epoch that achieves the best validation performance.

Next, we explore the effects of target-specific training on the training process and decoding performance. Fig. 5 shows the evolution of BLERs at signal-to-noise ratio (SNR) 1.4 dB for NWDs with various target sizes. As the target size  $T$  decreases, continuous improvements on performance occur, resulting in better performance convergence. This indicates that target-specific training facilitates more effective learning and achieves superior decoding performance compared to all-inclusive training, even though it uses a simpler network with

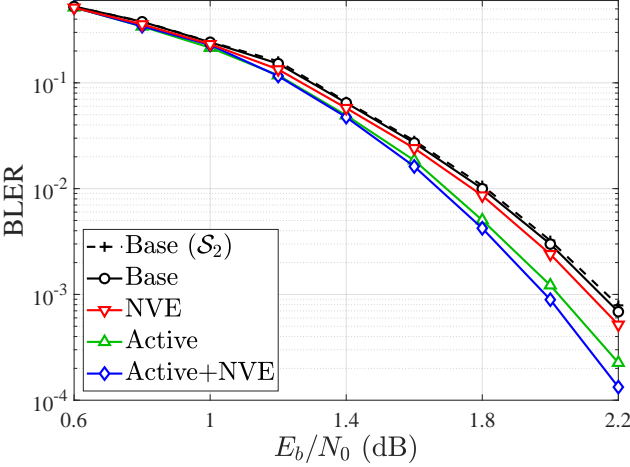


Fig. 6. BLER performance for the SC-LDPC code with  $z = 100$  and the NWD with  $W = 10$ ,  $\bar{\ell} = 10$ . The NWDs are trained using the conventional method (Conv), normalized loss (Norm Loss), active learning (Active), and both methods combined (Prop). Training data are collected from  $\mathcal{S}_1$ , except for Conv using  $\mathcal{S}_2$ .

In practice, training with equal per-SNR sample counts biases the model toward low-SNR data. Since errors—and thus nonzero BLER loss—are more frequent at low SNRs, their gradients dominate those at high SNRs. While the fixed structural pruning of the NWD offers several advantages, it can degrade training stability [41]. Indeed, as shown in Fig. 6, the NWD exhibits a pronounced training bias toward low-SNR data. The NWD trained on five SNR points,  $\mathcal{S}_1 = \{0.6, 1.0, 1.4, 1.8, 2.2\}$ , performs almost identically to that trained only on the two lowest points,  $\mathcal{S}_2 = \{0.6, 1.0\}$ .

To address these drawbacks of the pruned NWD, we adopt the active learning strategy from [10]. In this approach, mini-batches consist solely of error samples, which are received words that the decoder currently fails to decode, collected from each SNR. Because the BLER loss for these samples is always 1, each SNR contributes an equal total loss, resulting in balanced gradient updates. Additionally, we use the normalized validation error (NVE) [6] to fairly evaluate each epoch’s weights across multiple SNRs during validation.

Fig. 6 compares the performance of NWDs trained with different strategies. The result shows that active learning yields the largest BLER improvement, while NVE offers a smaller but still noticeable gain—likely because it is applied only during validation. When combined, the two techniques enhance training stability across a broad SNR range and yield the best overall performance. Importantly, these benefits are not limited to the NWD, but also apply to other neural decoders whose optimal weights vary across SNRs.

### C. Performance Results of the NWD

Based on the methods discussed in the previous subsections, we train the NWD with  $\bar{\ell} = 10$ ,  $W = 10$  for the SC-LDPC code with  $z = 100$ . We apply graph-based CN weight sharing and actively collect 20 error samples from each of 5 SNR points in  $\mathcal{S} = \{1.2, 1.4, 1.6, 1.8, 2.0\}$  to form mini-batches

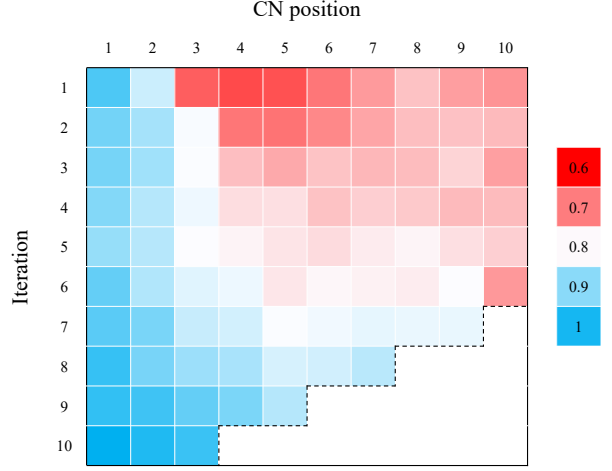


Fig. 7. Distribution of trained CN weights in NWD with  $T = 1$  target-specific training by CN position and iteration. The small weights (red) signify that the corresponding CN messages have relatively low reliability.

of size 100. Each epoch consists of 10 mini-batches, and the validation phase begins after the training of each epoch is completed. The validation score is computed using NVE, evaluated on 50000 samples, 10000 from each SNR point. After conducting training and validation for 1000 epochs, the NWD with the lowest NVE is selected.

Fig. 7 shows the distribution of trained weights in the NWD with  $T = 1$  target-specific training. The empty region under the dotted line represents pruned weights that are not connected to target nodes, reducing the number of weights by 16%. The small weights colored in red indicate that the associated CN messages are relatively unreliable. Larger weights correspond to more reliable CNs, which are located near the target position and in later decoding iterations. Within a window, low-degree front CNs are initially more reliable than high-degree rear CNs, and overall CN reliability increases with each iteration.

However, when focusing on the early iterations, the weights of middle CNs are lower than those of the rear CNs (see CN positions 3–10 in iteration 1). This is because unreliable initial messages from high-degree rear CNs require more than two iterations to reach the target nodes, during which their reliability improves. In contrast, unreliable messages from middle CNs are passed directly to the target nodes in early iterations, causing a more negative impact on decoding performance.

Finally, Fig. 8(a) shows the single-window BLER for the conventional WD using MS with a fixed weight 0.75, NWDs using the neural MS, and the conventional WD using BP. The result shows that the NWD with target-specific training achieves a 0.1 dB gain at  $\text{BLER} = 3 \times 10^{-4}$  compared to the WD, and also outperforms the NWD with all-inclusive training, despite using fewer weights. Furthermore, it matches the performance of the WD with the BP algorithm while requiring significantly lower computational complexity.

Next, we evaluate the decoders using sliding window decoding on the entire SC-LDPC code chain of length  $Ln = 20000$

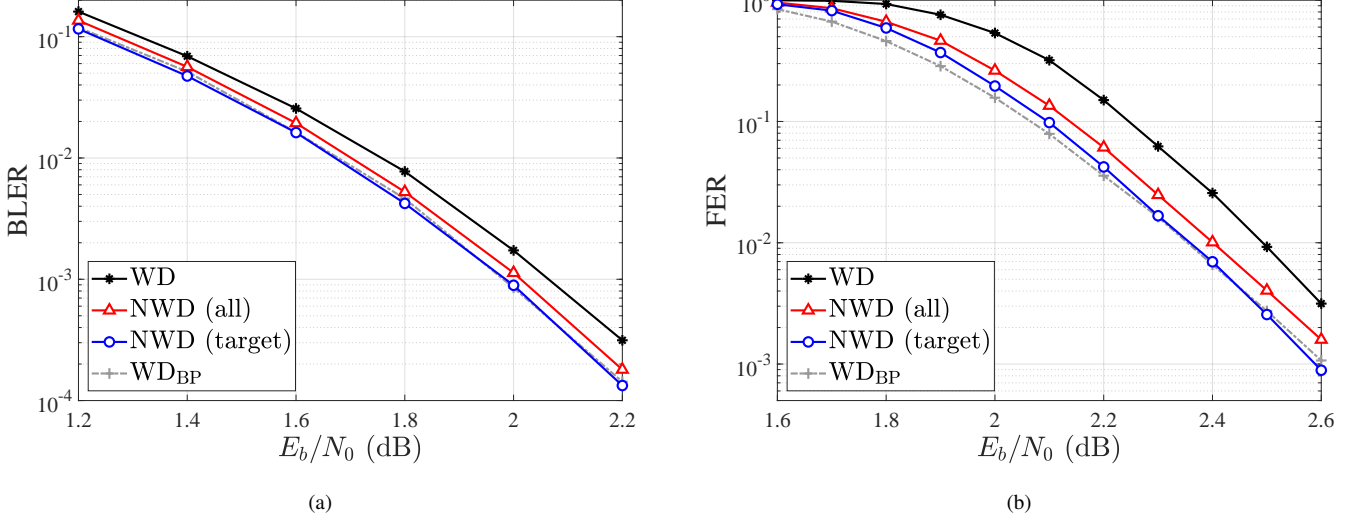


Fig. 8. (a) BLER performances of a single window block and (b) FER performances of the  $L_n = 20000$  SC-LDPC code for the conventional WD, the NWD with all-inclusive training, the NWD with  $T = 1$  target-specific training, and the conventional WD with the BP algorithm.

and present the FER in Fig. 8(b). As decoding progresses along the  $L = 100$  chain, the performance gap between decoders becomes more pronounced, yielding a larger FER difference than in BLER. The NWD with target-specific training achieves more than a threefold reduction in FER at  $E_b/N_0 = 2.5$  dB compared to the WD, and again outperforms the NWD with all-inclusive training. At high SNRs, it even attains a lower FER than the WD with BP.

This result also highlights that the weights of the NWD are effective even for long SC-LDPC codes of length 20000—a regime in which training a neural decoder on block codes becomes computationally infeasible—despite the fact that the weights are trained within a window that is independent of the overall code length.

#### IV. NEURAL NON-UNIFORM SCHEDULES FOR THE NWD

In this section, we propose a systematic method to optimize the non-uniform schedule of the NWD based on its training result. In a non-uniform schedule, certain CNs skip updating their messages; instead, they forward the output from the previous iteration.

##### A. Damping Factor and Schedule Importance

Identifying which CNs to be skipped based solely on the trained CN weights  $w_C^{(\ell)}$  is difficult, as these weights reflect message reliability rather than the significance of the updates themselves. To address this, we introduce damping factors [15], [42] into the NWD that directly indicate the importance of each update. Damping forms the current message by mixing the new update  $m_{c \rightarrow v}^{(\ell)}$  with the previous message  $m_{c \rightarrow v}^{(\ell-1)}$ . Accordingly, the damped CN message is obtained by applying damping to the CN update  $m_{c \rightarrow v}^{(\ell)}$  in (2) as follows:

$$m_{c \rightarrow v}^{(\ell)} \leftarrow \gamma_C^{(\ell)} m_{c \rightarrow v}^{(\ell-1)} + (1 - \gamma_C^{(\ell)}) m_{c \rightarrow v}^{(\ell)}, \quad (4)$$

where  $0 \leq \gamma_C^{(\ell)} \leq 1$  denotes the *damping factor* for proto CN  $C$  at iteration  $\ell$ . In the damped NWD, the damping factors  $\gamma_C^{(\ell)}$  are introduced as trainable parameters along with the CN weights  $w_C^{(\ell)}$ . As seen in (4), a larger damping factor implies that assigning greater weight to the previous-iteration message is beneficial for decoding. Since a CN update is replaced by previous message when  $\gamma_C^{(\ell)} = 1$ , skipping CNs with large  $\gamma_C^{(\ell)}$  is expected to have minimal impact on decoding performance. To encourage many  $\gamma_C^{(\ell)}$  values to approach 1, we add an  $\ell_1$  regularization term,  $\lambda \sum |1 - \gamma_C^{(\ell)}|$ , to the loss of the damped NWD, with  $\lambda$  set to 0.1 [43].

Fig. 9(a) shows the distribution of the trained  $\gamma_C^{(\ell)}$  values. In the early iterations (1 to 5), most  $\gamma_C^{(\ell)}$  values are concentrated in the range of 0–0.1 (colored blue to white), suggesting that the corresponding CN updates are essential. In later iterations (iterations 7–10), higher  $\gamma_C^{(\ell)}$  values (red) emerge, consistent with update saturation. Although the trained  $\gamma_C^{(\ell)}$  values reflect the importance of the CN updates, the prevalence of many similarly small values makes it difficult to clearly determine which CNs to be skipped.

Therefore, we propose a new metric, termed *schedule importance*, denoted  $\bar{\gamma}_C^{(\ell)} := \gamma_C^{(\ell)} / \bar{N}_C^{(\ell)}$ . In SC-LDPC codes, the impact of CN update skipping on the target VNs depends strongly on the distance to the target VNs. To capture this effect, we compute the number of paths  $N_C^{(\ell)}$  by which each CN can reach the target VNs at the last iteration in the expanded trellis graph across iterations. For example, the first CN at iteration 9 has 6 paths to the target VNs at iteration 10 in the trellis graph, which means  $N_1^{(9)} = 6$ . These counts are then normalized within each iteration to obtain normalized count  $\bar{N}_C^{(\ell)}$ , which represents the relative influence of each CN update on the target VNs. The distribution of  $\bar{N}_C^{(\ell)}$  is shown in Fig. 9(b).

Using this normalized reach count, we compute the schedule importance  $\bar{\gamma}_C^{(\ell)} = \gamma_C^{(\ell)} / \bar{N}_C^{(\ell)}$ , as shown in Fig. 9(c). CNs

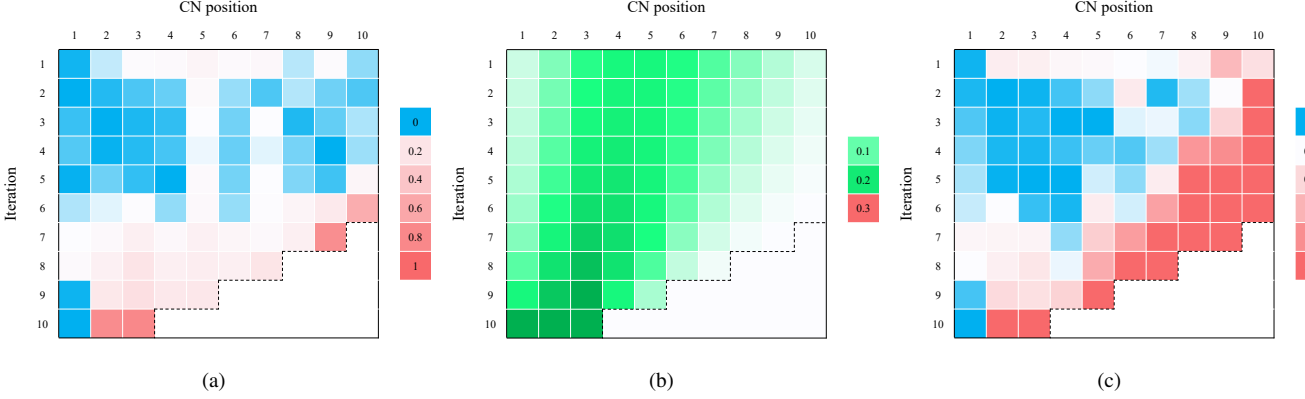


Fig. 9. (a) Distribution of trained damping factors  $\gamma$ , (b) normalized target reach counts  $\bar{N}$ , and (c) schedule importance  $\bar{\gamma}$ . CN updates with a high  $\bar{\gamma}$  (red) are considered to be skipped.

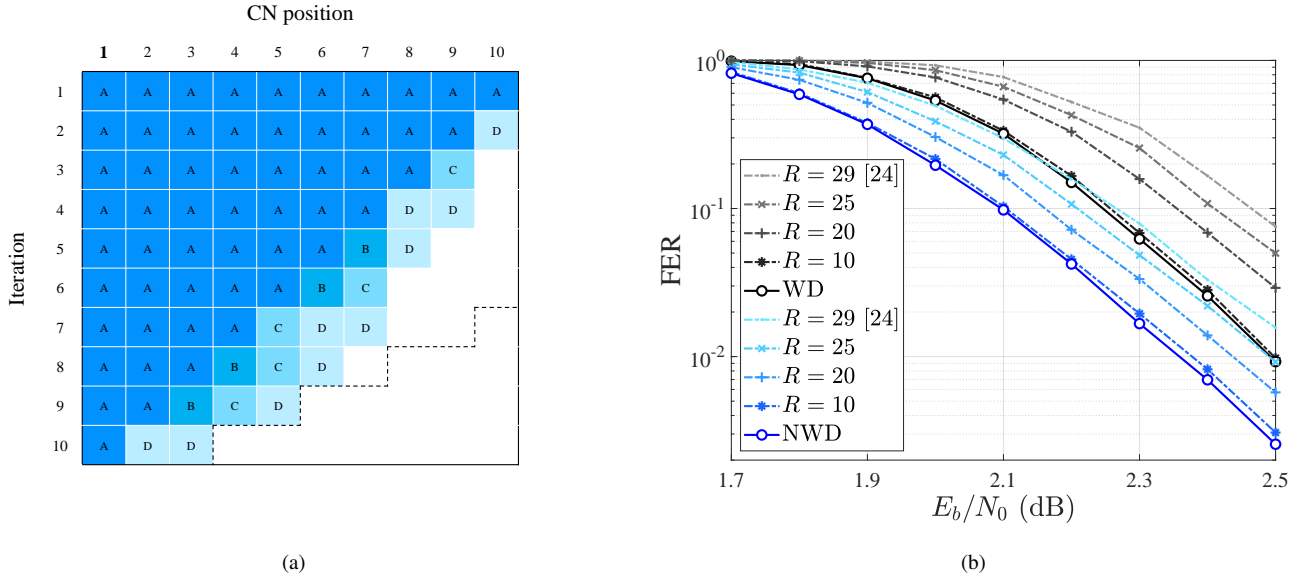


Fig. 10. (a) Non-uniform schedules based on the training results of the NWD: the points marked with A, A+B, A+B+C, and A+B+C+D indicate the active CN updates when skipping 29, 25, 20, and 10 CN updates, respectively. (b) FER performances with proposed neural non-uniform schedules applied to the WD and NWD.

with high  $\bar{\gamma}_C^{(\ell)}$  are considered strong candidates for skipping. Comparing Fig. 9(a) and (c), later-index CNs within each iteration (e.g., iteration 4 and CN index 9), which have relatively large damping factors  $\gamma_C^{(\ell)}$ , are more likely to be skipped because they have fewer paths to the target VNs and thus have higher  $\bar{\gamma}_C^{(\ell)}$ . Skipping such low-importance CN updates has minimal impact on the reliability of the target VNs and therefore incurs little performance degradation.

### B. Proposed Non-Uniform Schedules of the NWD

We skip CN updates one by one according to the following procedure. First, we collect the schedule importance values  $\bar{\gamma}_C^{(\ell)}$  from the last active iterations at each position. Then, at each step, we skip the CN update with the largest  $\bar{\gamma}_C^{(\ell)}$ . The resulting schedules are shown in Fig. 10(a) for the cases where 29, 25, 20, and 10 CN updates are skipped. In the figure, points marked with the symbol A indicate the active updates when

29 updates are skipped, while A+B marks the active updates when 25 CNs are skipped, and so on.

We determine the schedules based on the trained damping factors of the damped NWD. However, decoding with damping  $\gamma_C^{(\ell-1)}$  requires additional memory to store previous messages  $m_{c \rightarrow v}^{(\ell-1)}$  as described in Eq. (4). This additional cost can offset the complexity savings gained from scheduling. Therefore, we employ the damped NWD only to determine the schedule, while the actual decoding is performed by the plain NWD with the established schedule. In practice, the performance of the plain NWD under the proposed schedule is nearly indistinguishable from that of the damped NWD. Hence, the scheduling introduces no runtime overhead and allows the NWD to fully benefit from reduced complexity.

Fig. 10(b) presents the FER of the NWD and WD using the schedules in Fig. 10(a). For the NWD, the schedule with 10 inactive CNs, yielding a 26% reduction in CN updates, incurs almost no performance loss. Moreover, the schedule with 25 inactive CNs even outperforms the conventional WD,

suggesting that the NWD with appropriate scheduling can achieve equal or better performance than the conventional decoder while omitting up to 41% of CN updates. For the WD, performance degradation is minimal up to 10 inactive CNs, but beyond that, it experiences greater performance degradation than the NWD. Since the proposed scheduling depends on the NWD's trained weights, it is less effective for the WDs with fixed weights.

Note that the schedule with 29 inactive CNs coincides with the pragmatic schedule in [26]. The pragmatic schedule provides only a single scheduling option, which may lead to performance loss as shown in Fig. 10(b). In contrast, the proposed method offers multiple options along the complexity-performance trade-off. Furthermore, the method is not limited to SC-LDPC codes and can be applied to other codes with structural asymmetry.

## V. ADAPTIVE NWD FOR MITIGATING ERROR PROPAGATION

In this section, we propose an adaptive NWD scheme to mitigate EP in the NWD. Previous training methods used the independent window configuration, where it is assumed that all preceding target nodes are correctly decoded. Consequently, the earliest nodes in each window are treated as the most reliable. When EP occurs, however, errors from earlier windows make these front-end nodes the least reliable, rendering the weights trained under the independent window assumption ineffective. While NWD performs well under EP-free conditions, it becomes vulnerable once EP begins; the proposed adaptive scheme addresses this limitation.

The general Markov decoder model for window decoding [29] shows that it becomes increasingly difficult to recover from EP as the decoder progresses into deeper EP states. Thus, a simple yet effective strategy is to intervene as soon as an error is detected in the previous stage. We focus on the Markov model with  $J = 1$  and aim to reduce the probability  $q_1$  of an error occurring in the current block given that an error has occurred in the previous block. We refer to  $q_1$  as the EP probability.

### A. Training Method for the EP-resilient Weight Set

We propose an adaptive NWD scheme that uses the plain weight set  $w_{c_p}^{(\ell)}$  and switches to an *EP-resilient weight set*  $\bar{w}_{c_p}^{(\ell)}$  when an error is detected in the previous stage. While the plain weight set  $w_{c_p}^{(\ell)}$  is trained under an independent window configuration, the EP-resilient weight set  $\bar{w}_{c_p}^{(\ell)}$  is trained under a connected window configuration that includes previously decoded VNs connected to the front CNs, as shown in Fig. 11. This configuration accounts for error propagation scenarios from the previous stage.

To train  $\bar{w}_{c_p}^{(\ell)}$ , we use a boosting learning technique [12], [13], which selectively collects uncorrected codewords from the previous decoder in a multi-stage decoding setup. Similarly, we collect training data from the case where the previous window fails, regardless of the decoding results of the current window. For example, as shown in Fig. 11, if the 50th window fails, we collect the decision LLRs of target VNs in the 50th

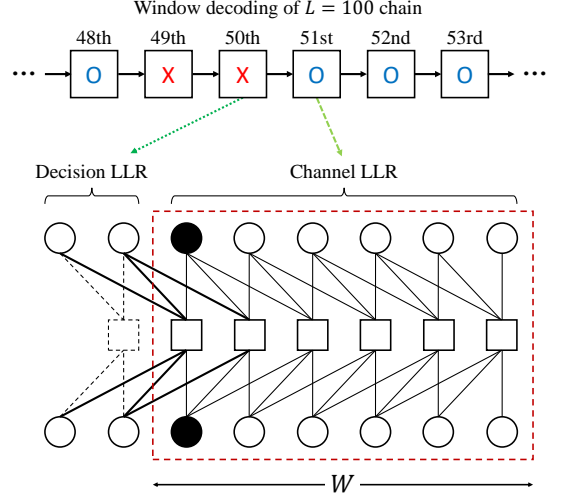


Fig. 11. Training method for the EP-resilient weight set. When an error occurs in the previous block (50th), the decision LLRs of the target VNs from the previous block and the channel LLRs of all VNs in the current block (51st) are collected as training data for the EP-resilient weight set.

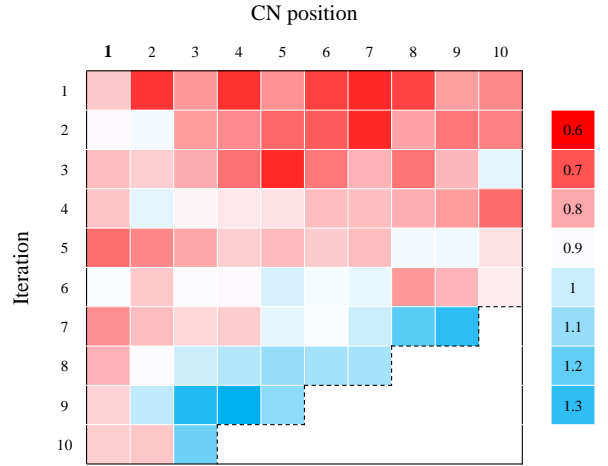


Fig. 12. Distribution of the trained EP-resilient weight set.

window and the channel LLRs of all VNs in the 51st window. We collect 5000 samples at an SNR point of 2.0 dB, and train over 500 epochs. The initial weights are set to the plain weight set  $w_{c_p}^{(\ell)}$ . After training, the EP probability reduces from 0.781 to 0.642, demonstrating that the EP-resilient weight set clearly improves robustness to EP.

The distribution of  $\bar{w}_{c_p}^{(\ell)}$  is depicted in Fig. 12. Compared to the distribution of the plain weight set  $w_{c_p}^{(\ell)}$  in Fig. 7, the weights of the front CNs are significantly smaller, reflecting unreliable incoming messages. Conversely, in later iterations, the weights for mid-to-rear CNs exceed 1, indicating that messages from the relatively more reliable rear nodes are amplified to help correct errors propagated from the front.

### B. Proposed Adaptive NWD Scheme

The adaptive NWD should first detect errors in the previous window. This is done by inspecting the parity-check equations

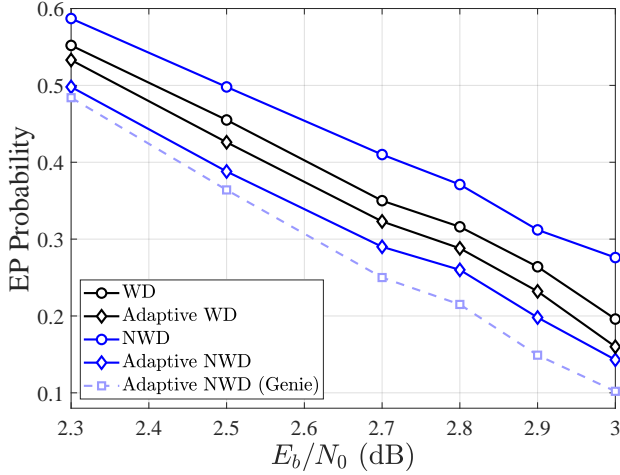


Fig. 13. EP probabilities for the WD, NWD, and adaptive NWD. The adaptive decoder detects previous block errors using the parity check status of the previous CNs or a genie-aided method (Genie).

that involve only the previously decoded target VNs (dashed square in Fig. 11). If any CN is unsatisfied, referred to as an unsatisfied CN (UCN), it indicates a prior error and triggers the use of the EP-resilient weight set for the current window. By the symmetric structure of SC-LDPC codes, the presence of a UCN indicates an odd-parity mismatch among the earlier target VNs, which implies at least one error. For reference, we also evaluate an ideal, genie-aided detector.

Fig. 13 shows the average EP probability across all window blocks for the WD, NWD, and adaptive NWD. Compared with the WD, the NWD shows a higher EP probability. This gap becomes more pronounced at high SNRs where the discrepancy in decoder inputs between EP and EP-free cases is larger [29]. This result confirms that the NWD is more vulnerable to EP than the WD. Unlike the WD, which applies uniform weights across all positions, the NWD assumes perfect decoding in the previous block and assigns higher weights to the front positions, as in Fig. 7. Consequently, in the presence of EP, the NWD amplifies errors from the previous block, leading to an increased probability of block decoding failure.

In contrast, the adaptive NWD with the UCN-based error detector markedly suppresses EP, achieving a lower EP probability than the conventional WD. When the detector is ideal, as in the genie-aided case, the EP reduction is even more substantial. For comparison, we also evaluate an adaptive WD that switches between a fixed weight and the EP-resilient weight set based on the detected error status. However, the error patterns encountered during the adaptive WD decoding differ from those used to train the EP-resilient weights, yielding only a modest reduction in EP, substantially less than that achieved by the adaptive NWD.

Finally, we compare the average BLER for the SC-LDPC code with code length  $Ln = 100 \times 200 = 20000$  using various decoders in Fig. 14. Compared with the WD, the NWD shows a more gradual BLER slope at high SNRs due to its higher EP probability at high SNRs. However, the adaptive NWD scheme reduces EP probability and restores the BLER slope

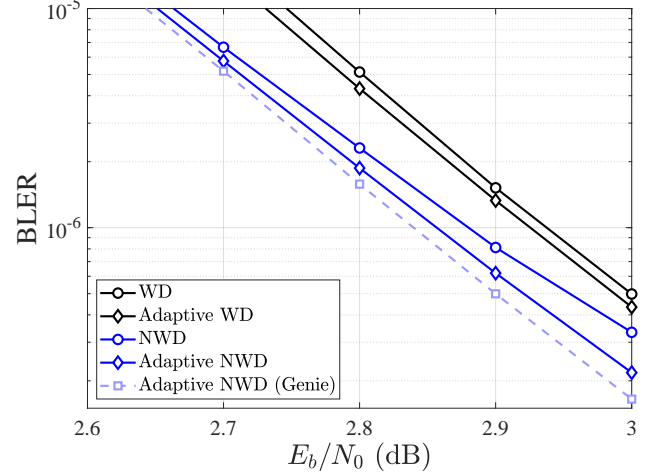


Fig. 14. Average BLER performances of the  $Ln = 20000$  SC-LDPC code for the WD, NWD, and adaptive decoders.

at high SNRs to a level comparable to the slope of the WD.

In addition, the adaptive NWD scheme offers practical implementation advantages. Unlike previous EP mitigation methods that require code modifications [29] or online BER estimation [27], the proposed scheme requires only storing an additional weight set in memory. Furthermore, since the decoder already checks CN satisfaction at each iteration for early stopping, the UCN-based detector incurs no additional latency or computational overhead, as it leverages this existing information.

## VI. COMPLEXITY ANALYSIS OF PROPOSED NWDs

Table I compares the computational complexity of the proposed NWDs and conventional decoders for a single window of the  $(3, 6)$ -regular SC-LDPC code. We count all elementary operations involved in window decoding, including additions, comparisons, sign multiplications, weight multiplications, and the table lookups for tanh operations. As shown in Fig. 10(a), the NWD skips certain node and edge operations, and therefore requires fewer operations than the WD. For instance, the WD using the fixed-weight MS algorithm carries out  $E\bar{\ell} = 540$  weight multiplications, whereas the NWD reduces this to 444. Skipping 25 CN updates using the neural non-uniform schedule lowers the count further to 296.

To evaluate the decoding complexity on modern processors, we follow the Horowitz energy model [44], in which a floating-point addition costs about 0.9 pJ, a multiplication about 3.7 pJ, and an on-chip SRAM access about 5 pJ. Normalizing the addition to 1 unit, we count a comparison as 1 unit because CMP is realized as a subtraction on the same ALU datapath [45]. A sign multiplication, realized as a sign-bit flip/XOR, is counted as 0.3 units [46]. A variable weight multiplication is counted as 4 units, and a table lookup—including the SRAM fetch and a small interpolation step—is counted as 6 units.

First, comparing complexity across NWD training methods confirms that target-specific training uses fewer weights and reduces decoding complexity by 18% while achieving a lower

TABLE I  
COMPLEXITY COMPARISON OF WINDOW DECODERS FOR THE SC-LDPC CODE OF  $(N, M, z, \bar{\ell}) = (20, 10, 100, 10)$ , WHERE  $\alpha$  IS THE COMPARISON COUNT FOR EACH CN (I.E.,  $\alpha = d_c + \lceil \log d_c \rceil - 2$  FOR THE CN DEGREE  $d_c$  [47])

	Complexity per protograph					Total Complexity ( $A + C + 0.3S + 4W + 6T$ ) $z$ )	Number of weights	FER @ 2.5 dB	BLER @ 3.0 dB
	Addition $A = 2E\bar{\ell}$	Comparison $C = \alpha M\bar{\ell}$	Sign mul. $S = 2E\bar{\ell}$	Weight mul. $W = E\bar{\ell}$	LUT $T = 2E\bar{\ell}$				
WD <sub>BP</sub>	1080	0	1080	0	1080	788400 (+89%)	0	2.74E-03	3.91E-07
WD	1080	610	1080	540	0	<b>417400 (-)</b>	1	<b>9.25E-03</b>	<b>4.98E-07</b>
NWD (all)	1080	610	1080	540	0	417400 (-)	100	4.04E-03	4.32E-07
NWD (target)	888	498	888	444	0	342840 (-18%)	84	<b>2.56E-03</b>	3.33E-07
NWD, $R = 25$	592	326	592	296	0	227960 ( <b>-45%</b> )	59	9.20E-03	2.71E-06
Adaptive NWD	888	498	888	444	0	342840 (-18%)	168	2.56E-03	<b>2.18E-07</b>

FER. Remarkably, the NWD (target) achieves a threefold reduction in FER even at lower complexity than the WD. Furthermore, the NWD (target) even outperforms BP window decoding, despite its significantly lower complexity. The only overhead incurred by the neural decoder is memory for weight storage. With protograph CN sharing, the required weight count is  $MW \times \bar{\ell} = 100$ , and target-specific training further reduces it to 84.

Next, applying a neural non-uniform schedule with  $R = 25$  reduces the complexity by 45% and the number of weights to 59 while maintaining similar FER to the WD. Finally, the adaptive NWD designed to mitigate EP maintains the same decoding complexity as the plain NWD, since the error detection process requires no additional operations. The only additional cost is the memory required to store the EP-resilient weight set, which increases the number of stored weights to  $84 \times 2 = 168$ . Consequently, the adaptive NWD achieves a 35% reduction in BLER compared with the NWD with negligible resource overhead.

## VII. CONCLUSION

In this paper, we presented the first neural decoder for SC-LDPC codes, named NWD, which achieves improved decoding performance with reduced complexity. The NWD employs a target-specific training approach that significantly decreases the number of trainable weights, thereby lowering both decoding complexity and memory requirements and consequently improving decoding performance. Furthermore, we proposed a neural non-uniform schedule derived from the training results, which maintains performance comparable to the WD while reducing decoding complexity by 45%. In addition, an adaptive version of NWD was introduced, which dynamically selects the appropriate weight set based on the status of the previous block. This adaptive mechanism reduces both EP probability and BLER without modifying the original code or decoder architecture.

Overall, the proposed methods are hardware-friendly and introduce negligible runtime overhead, as they only require loading trained weights into an existing decoder. From the perspective of training complexity, the NWD can be efficiently trained with a small window configuration and subsequently applied to decode practical, long SC-LDPC codes. These advantages suggest that the NWD can enhance the overall performance of SC-LDPC codes and expand their applicability in practical communication systems.

## REFERENCES

- [1] H. He, C.-K. Wen, S. Jin, and G. Y. Li, “Deep learning-based channel estimation for beamspace mmWave massive MIMO systems,” *IEEE Wireless Commun. Lett.*, vol. 7, no. 5, pp. 852–855, Oct. 2018.
- [2] T. O’Shea and J. Hoydis, “An introduction to deep learning for the physical layer,” *IEEE Trans. Cognitive Commun. Netw.*, vol. 3, no. 4, pp. 563–575, Dec. 2017.
- [3] K. Muah, R. Fritschek, and R. F. Schaefer, “Learning end-to-end channel coding with diffusion models,” in *26th International ITG Workshop on Smart Antennas and 13th Conference on Systems, Communications, and Coding (WSA & SCC 2023)*, 2023, pp. 1–6.
- [4] W. R. Caid and R. W. Means, “Neural network error correcting decoders for block and convolutional codes,” in *Proc. IEEE Global Telecommunications Conference and Exhibition (GLOBECOM)*, 1990, pp. 1028–1031.
- [5] L. G. Tallini and P. Cull, “Neural nets for decoding error-correcting codes,” in *Proc. IEEE Tech. Appl. Conf. Workshops*, 1995, pp. 89.
- [6] T. Gruber, S. Cammerer, J. Hoydis, and S. ten Brink, “On deep learning-based channel decoding,” in *Proc. Annu. Conf. Inf. Sci. Syst. (CISS)*, 2017, pp. 1–6.
- [7] T. Matsumine, and O. Hideki, “Recent advances in deep learning for channel coding: A survey,” in *IEEE Open Journal of the Communications Society*, Oct. 2024, pp. 6443–6481.
- [8] E. Nachmani, Y. Be’ery, and D. Burshtein, “Learning to decode linear codes using deep learning,” in *Proc. 54th Annu. Allerton Conf. Commun., Control, Comput.*, Sep. 2016, pp. 341–346.
- [9] E. Nachmani, and L. Wolf, “Hyper-graph-network decoders for block codes,” *Advances in Neural Information Processing Systems*, vol. 32, 2019.
- [10] I. Be’ery, N. Raviv, T. Raviv, and Y. Be’ery, “Active deep decoding of linear codes,” *IEEE Trans. Commun.*, vol. 68, no. 2, pp. 728–736, 2020.
- [11] A. Buchberger, C. Hager, H. D. Pfister, L. Schmalen, and A. Graell I Amat, “Pruning and quantizing neural belief propagation decoders,” *IEEE J. Sel. Areas Commun.*, vol. 39, no. 7, pp. 1957–1966, 2020.
- [12] H. Y. Kwak, D. Y. Yun, Y. Kim, S. H. Kim, and J. S. No, “Boosting Learning for LDPC Codes to Improve the Error-Floor Performance,” *Advances in Neural Information Processing Systems (NeurIPS)*, vol. 36, 2024.
- [13] H. Y. Kwak, D. Y. Yun, Y. Kim, S. H. Kim, and J. S. No, “Boosted Neural Decoders: Achieving Extreme Reliability of LDPC Codes for 6G Networks,” *IEEE J. Sel. Areas Commun.*, vol. 43, no. 4, pp. 1089–1102, 2025.
- [14] E. Nachmani, E. Marciano, D. Burshtein, and Y. Be’ery, “RNN decoding of linear block codes,” 2017, *arXiv:1702.07560*.
- [15] M. Lian, F. Carpi, C. Häger, and H. D. Pfister, “Learned belief-propagation decoding with simple scaling and SNR adaptation,” in *Proc. IEEE Int. Symp. Inf. Theory (ISIT)*, Jul. 2019, pp. 161–165.
- [16] J. Dai, K. Tan, Z. Si, K. Niu, M. Chen, H. V. Poor, and S. Cui, “Learning to decode protograph LDPC codes,” *IEEE Journal on Selected Areas in Communications*, vol. 39, no. 7, pp. 1983–1999, May 2021.
- [17] L. Wang, C. Terrill, D. Divsalar, and R. D. Wesel, “LDPC decoding with degree-specific neural message weights and RCQ decoding,” *IEEE Trans. Commun.*, vol. 72, no. 4, pp. 1912–1924, Apr. 2024.
- [18] X. Chen and M. Ye, “Cyclically equivariant neural decoders for cyclic codes,” in *Proc. International Conference on Machine Learning (ICML)*, 2021.
- [19] N. Shah and Y. Vasavada, “Neural layered decoding of 5G LDPC codes,” *IEEE Commun. Lett.*, vol. 25, no. 11, pp. 3590–3593, 2021.

[20] H. Y. Kwak, J. W. Kim, Y. Kim, S. H. Kim, and J. S. No, “Neural Min-Sum Decoding for Generalized LDPC Codes,” *IEEE Commun. Lett.*, vol. 26, no. 12, pp. 2841–2845, 2022.

[21] W. Xu, X. Tan, Y. Be’ery, Y. L. Ueng, Y. Huang, X. You, and C. Zhang, “Deep learning-aided belief propagation decoder for polar codes,” *IEEE Journal on Emerging and Selected Topics in Circuits and Systems*, vol. 10, no. 2, pp. 189–203, 2020.

[22] A. Jiménez Felström and K. S. Zigangirov, “Time-varying periodic convolutional codes with low-density parity-check matrix,” *IEEE Trans. Inf. Theory*, vol. 45, no. 6, pp. 2181–2191, Sep. 1999.

[23] S. Kudekar, T. J. Richardson, and R. L. Urbanke, “Threshold saturation via spatial coupling: why convolutional LDPC ensembles perform so well over the BEC,” *IEEE Trans. Inf. Theory*, vol. 57, no. 2, pp. 803–834, Feb. 2011.

[24] A. R. Iyengar, M. Papaleo, P. H. Siegel, J. K. Wolf, A. Vanelli-Coralli, and G. E. Corazza, “Windowed decoding of protograph-based LDPC convolutional codes over erasure channels,” *IEEE Trans. Inf. Theory*, vol. 58, no. 4, pp. 2303–2320, Apr. 2012.

[25] H. Y. Kwak, J. W. Kim, H. Park, and J. S. No, “Optimization of SC-LDPC codes for window decoding with target window sizes,” *IEEE Trans. Commun.*, vol. 70, no. 5, pp. 2924–2938, 2022.

[26] N. UI Hassan, A. E. Pusane, M. Lentmaier, G. P. Fettweis, and D. J. Costello, Jr., “Non-uniform window decoding schedules for spatially coupled LDPC codes,” *IEEE Trans. Commun.*, vol. 65, no. 2, pp. 501–510, Feb. 2017.

[27] K. Klaiber, S. Cammerer, L. Schmalen, and S. ten Brink, “Avoiding burst-like error patterns in windowed decoding of spatially coupled LDPC codes,” in *Proc. IEEE 10th Int. Symp. on Turbo Codes & Iterative Inf. Processing*, Dec. 2018, pp. 1–5.

[28] O. Griebel, B. Hammoud, and N. Wehn, “Adaptive Sliding Window Decoding of Spatially Coupled LDPC Codes: Algorithms and Energy-Efficient Implementations,” in *IEEE Access*, Dec. 2024, pp. 191140–191161.

[29] M. Zhu, D. G. M. Mitchell, M. Lentmaier, D. J. Costello, Jr., and B. Bai, “Error propagation mitigation in sliding window decoding of spatially coupled LDPC codes,” *IEEE Journal on Selected Areas in Information Theory*, pp. 470–486, Sep. 2023.

[30] M. Zhu, D. G. M. Mitchell, M. Lentmaier, D. J. Costello, Jr., and B. Bai, “Combating error propagation in window decoding of braided convolutional codes,” in *Proc. IEEE International Symposium on Information Theory (ISIT)*, Jun. 2018, pp. 1380–1384.

[31] M. Zhu, D. G. M. Mitchell, M. Lentmaier, D. J. Costello, Jr., and B. Bai, “Error propagation mitigation in sliding window decoding of braided convolutional codes,” *IEEE Trans. Commun.*, vol. 68, no. 11, pp. 6683–6698, Nov. 2020.

[32] D. G. M. Mitchell, M. Lentmaier, and D. J. Costello, Jr., “Spatially coupled LDPC codes constructed from protographs,” *IEEE Trans. Inf. Theory*, vol. 61, no. 9, pp. 4866–4889, Jul. 2015.

[33] E. Sharon, N. Presman, and S. Litsyn, “Convergence analysis of generalized serial message-passing schedules,” *IEEE J. Sel. Areas Commun.*, vol. 27, no. 6, pp. 1013–1024, Aug. 2009.

[34] G. Elidan, I. McGraw, and D. Koller. (Jul. 2006), “Residual belief propagation: Informed scheduling for asynchronous message passing,” [Online]. Available: <https://arxiv.org/abs/1206.6837>

[35] A. I. V. Casado, M. Griot, and R. D. Wesel, “LDPC decoders with informed dynamic scheduling,” *IEEE Trans. Commun.*, vol. 58, no. 12, pp. 3470–3479, Dec. 2010.

[36] E. Nachmani, E. Marciano, L. Lugosch, W. J. Gross, D. Burshtein, and Y. Be’ery, “Deep learning methods for improved decoding of linear codes,” *IEEE J. Sel. Topics Signal Process.*, vol. 12, no. 1, pp. 119–131, Feb. 2018.

[37] D. Kingma, and J. Ba, “Adam: A method for stochastic optimization,” *arXiv preprint arXiv:1412.6980*, 2014

[38] J. Chen, A. Dholakia, E. Eleftheriou, M. P. C. Fossorier, and X.-Y. Hu, “Reduced-complexity decoding of LDPC codes,” *IEEE Trans. Commun.*, vol. 53, no. 8, pp. 1288–1299, Aug. 2005.

[39] X. Xiao, N. Raveendran, B. Vasic, S. Lin, and R. Tandon, “FAID diversity via neural networks,” in *Proc. 11th Int. Symp. Topics Coding (ISTC)*, Aug. 2021, pp. 1–5.

[40] K. Huang, D. G. M. Mitchell, L. Wei, X. Ma, and D. J. Costello, Jr., “Performance comparison of LDPC block and spatially coupled codes over  $GF(q)$ ,” *IEEE Trans. Commun.*, vol. 63, no. 3, pp. 592–604, Mar. 2015.

[41] Z. He, Z. Xie, Q. Zhu, and Z. Qin, “Sparse double descent: Where network pruning aggravates overfitting,” in *Proc. Int. Conf. Mach. Learn. (ICML)*, Jun. 2022, pp. 8635–8659.

[42] M. Fossorier, R. Palanki, and J. Yedidia, “Iterative decoding of multi-step majority logic decodable codes,” in *Proc. Int. Symp. on Turbo Codes and Related Topics*, 2003, pp. 125–132.

[43] J. H. Friedman, T. Hastie, and R. Tibshirani, “Regularization paths for generalized linear models via coordinate descent,” *Journal of Statistical Software*, vol. 33, no. 1, pp. 1–22, Feb. 2010.

[44] S. Han, X. Liu, H. Mao, J. Pu, A. Pedram, M. A. Horowitz, and W. J. Dally, “EIE: Efficient inference engine on compressed deep neural network,” *ACM SIGARCH Computer Architecture News*, vol. 44, no. 3, pp. 243–254, 2016.

[45] Intel Corporation, *Intel 64 and IA-32 Architectures Software Developer’s Manual, Vol. 3B: System Programming Guide, Part 2*, May 2011.

[46] A. Abel and J. Reineke, “uops.info: Characterizing latency, throughput, and port usage of instructions on Intel microarchitectures,” in *Proc. 24th Int. Conf. Archit. Support Program. Lang. Oper. Syst. (ASPLOS)*, Providence, RI, USA, 2019, pp. 673–686.

[47] W. Ryan and S. Lin, *Channel Codes: Classical and Modern*, Cambridge University Press, 2009.